where $a = 4.575 \times 10^{-3}$ kcal/mol, T = coalescence temperature (K), and k = rate constant (s^{-1}).

X-ray Crystallography. Dark green crystals of $(CH_3C_5H_4)_4Ti_4S_8O_2$ were grown from CH_2Cl_2 solutions layered with hexanes. A crystal with dimensions 0.22 × 0.30 × 0.38 mm was found to be trigonal with cell dimensions a = 10.700 (2) Å, c = 22.530 (6) Å, and V = 2233.9 (9) Å^3. The measured density of 1.75 g/cm^3 was in good agreement with the calculated density of 1.77 g/cm^3 for $Z = 3$. The data were collected on a Nicolet R3 automated diffractometer by using the ω-scan technique ($4° \le 2\theta \le 50°$) at ambient temperature with monochromatized Mo Kα (λ = 0.71069 Å) radiation, μ = 16.3 cm^{-1}. Of the 4271 reflections collected, 2633 were unique and 2619 were observed at the $(F_o) > 2.5\sigma(F_o)$ level of confidence. The structure was solved by direct methods in $P3_1$; after the presence of a 2-fold rotational symmetry became apparent, the coordinates were transformed to those for $P3_121$ (in $P3_221$, R = 0.0259). All non-hydrogen atoms were refined with anisotropic temperature factors; all methyl group hydrogen atoms were located and refined isotropically with ring hydrogen atoms placed in idealized positions. At convergence R = 0.0234, R_w = 0.0246, GOF = 0.935, mean Δ/σ = 0.09, and the highest residual peak = 0.34 e/Å^3. Atomic coordinates and anisotropic thermal parameters are presented in Table II.

Acknowledgment. This research was supported by the National Science Foundation and by fellowships to T.B.R. from the Camille and Henry Dreyfus Foundation. D. M. Giolando is thanked for his assistance in the early stages of this project. Field desorption mass spectra were obtained in the Mass Spectrometry Laboratory, School of Chemical Sciences, University of Illinois, supported in part by a grant from the National Institute of General Medical Sciences (Grant GM27029).

Registry No. 2, 101224-50-4; **2″**, 101224-51-5; $(CH_3C_5H_4)TiCl_3$, 1282-31-1; $LiHBEt_3$, 22560-16-3; Li_2S_2, 51148-09-5; $(C_5H_5)TiCl_3$, 1270-98-0.

Supplementary Material Available: Listings of complete bond lengths and angles, anisotropic thermal parameters, all hydrogen atom parameters, and structure factors (21 pages). Ordering information is given on any current masthead page.

Contribution from the Departments of Chemistry, Colorado State University, Fort Collins, Colorado 80523, and The University of North Carolina, Chapel Hill, North Carolina 27514, and Department of Physics, University of Vermont, Burlington, Vermont 05405

Synthesis of an Iron(III) Porphyrin Dimer with a *trans*-Dicyanoethylenedithiolate Bridging Ligand: Structural and Magnetic Studies on $(\mu$-FNT-*S*,*S*′)[Fe(TPP)]$_2$·2C$_6$H$_6$

C. Michael Elliott,*[1a] Kozo Akabori,[1b] Oren P. Anderson,*[1a] Cynthia K. Schauer,[1a] William E. Hatfield,*[1c] P. B. Sczaniecki,[1d] Samarash Mitra,[1e] and K. Spartalian*[1f]

Received July 16, 1985

An iron(III) porphyrin dimer containing a novel bridge involving the FNT^{2-} ligand (FNT^{2-} = *trans*-1,2-dicyanoethylenedithiolate) has been synthesized. A single-crystal X-ray diffraction study (monoclinic, $P2_1/n$, a = 14.263 (3) Å, b = 15.184 (4) Å, c = 19.172 (4) Å, β = 93.92 (2)°, $Z = 2$) of **1** ($(\mu$-FNT-*S*,*S*′)[Fe(TPP)]$_2$·2C$_6$H$_6$) shows that the iron(III) atoms of the centrosymmetric dimer are axially bonded to the trans sulfur atoms of the planar FNT^{2-} bridging ligand (Fe–S = 2.324 (2) Å). The plane of the bridging ligand is nearly parallel to the porphyrin plane, implying that the iron atoms interact with π electrons of the FNT^{2-} bridge. The metric parameters for the [Fe(TPP)]$^+$ unit indicate high-spin character for the iron atoms. The magnetic susceptibility of **1** is matched well between 1.8 K and room temperature by susceptibilities calculated from a theoretical model that includes antiferromagnetic coupling between two such high-spin iron(III) atoms; the best values of J and $|D|$ are −8.5 and 9.6 cm^{-1}, respectively. Mössbauer and EPR spectroscopic results for **1** support the high-spin assignment and antiferromagnetic coupling scheme.

Introduction

Bonds between the iron atom of an iron(III) porphyrin unit and axial thiolate ligands occur in a number of heme protein systems.[2] The ability of sulfur-containing ligands to mediate the electronic coupling between metal centers and to affect the spin state of individual iron(III) atoms is of considerable importance in understanding the biological role of these sulfur-ligated heme units. However, only a small number of systems containing an iron(III) porphyrin with axial sulfur ligands have been prepared and structurally characterized,[3] in part because of the facile oxidation–reduction reaction that occurs between iron(III) and many sulfur-containing ligands of interest.

We have prepared a dimer of ferric porphyrins, in which bridging between the two iron(III) atoms is accomplished by binding of the iron atoms to the trans sulfur atoms of FNT^{2-} (FNT^{2-} = *trans*-1,2-dicyanoethylenedithiolate, or fumaronitriledithiolate). The structure and physical properties of this system ($(\mu$-FNT-*S*,*S*′)[Fe(TPP)]$_2$·2C$_6$H$_6$, hereafter **1**) constitute the subject of this report.

Experimental Section

Synthesis of (μ-*trans*-1,2-Dicyanoethylenedithiolato-*S*,*S*′)bis((tetraphenylporphinato)iron(III))–2-Benzene, (μ-FNT-*S*,*S*′)[Fe(TPP)]$_2$·2C$_6$H$_6$ (1). [Fe(TPP)(ClO$_4$)]·0.5C$_6$H$_5$CH$_3$[4] and sodium *trans*-1,2-dicyanoethylenedithiolate (Na_2FNT)[5,6] were prepared by literature methods. A mixture of [Fe(TPP)(ClO$_4$)]·0.5C$_6$H$_5$CH$_3$ (0.2056 g, 2.53×10^{-4} mol) and Na_2FNT (0.0958 g, 5.15×10^{-4} mol) in benzene (130 mL) was stirred at reflux temperature for 6 h, cooled to room temperature, and passed through a medium frit to separate excess solid Na_2FNT. *n*-Heptane (50 mL) was added to the filtrate slowly, with constant stirring. After reduction of solvent volume (to ca. 30 mL), fine purple-black crystals of **1** were collected on a medium frit, washed with *n*-heptane, weighed (0.1833 g, 89% yield), and analyzed. (Anal. Calcd for $C_{104}H_{68}N_{10}S_2Fe_2$: C, 76.47; H, 4.20; N, 8.57. Found: C, 76.66; H, 4.44; N, 8.83.) The solution spectrum in benzene is shown in Figure 1.

Single crystals of **1** of suitable size and quality for X-ray diffraction studies were grown by vapor diffusion of *n*-heptane into a solution of **1**

(1) (a) Colorado State University. (b) Present address: Faculty of Integrated Arts and Sciences, Hiroshima University, 1-1-89, Higashisenda, Naka-ku, Hiroshima, 730 Japan. (c) University of North Carolina. (d) Present address: Institute of Molecular Physics, Poznan, Poland. (e) Present address: Tata Institute for Fundamental Research, Bombay, India. (f) University of Vermont.

(2) Ibers, J. A.; Holm, R. H. *Science* (*Washington, D.C.*) **1980**, *209*, 223.

(3) (a) Mashiko, T.; Reed, C. A.; Haller, K. J.; Kastner, M. E.; Scheidt, W. R. *J. Am. Chem. Soc.* **1981**, *103*, 5758. (b) Tang, S. C.; Koch, S.; Papaefthymiou, G. C.; Foner, S.; Frankel, R. B.; Ibers, J. A.; Holm, R. H. *J. Am. Chem. Soc.* **1976**, *98*, 2414. (c) Caron, C.; Mitschler, A.; Rivière, G.; Ricard, L.; Schappacher, M.; Weiss, R. *J. Am. Chem. Soc.* **1979**, *101*, 7401. (d) Collman, J. P.; Sorrell, T. N.; Hodgson, K. O.; Kulshrestha, A. K.; Strouse, C. E. *J. Am. Chem. Soc.* **1977**, *99*, 5180. (e) Schappacher, M.; Ricard, L.; Weiss, R.; Montiel-Montoya, R.; Gonser, U.; Bill, E.; Trautwein, A. *Inorg. Chim. Acta* **1983**, *78*, L9. (f) English, D. R.; Hendrickson, D. N.; Suslick, K. S.; Eigenbrot, C. W., Jr.; Scheidt, W. R. *J. Am. Chem. Soc.* **1984**, *106*, 7258.

(4) Reed, C. A.; Mashiko, T.; Bentley, S. P.; Kastner, M. E.; Scheidt, W. R.; Spartalian, K.; Lang, G. *J. Am. Chem. Soc.* **1979**, *101*, 2948.

(5) Davison, A.; Holm, R. H. *Inorg. Synth.* **1967**, *10*, 8.

(6) Simmons, H. E.; Blomstrom, D. C.; Vest, R. D. *J. Am. Chem. Soc.* **1962**, *84*, 4756.

0020-1669/86/1325-1891$01.50/0

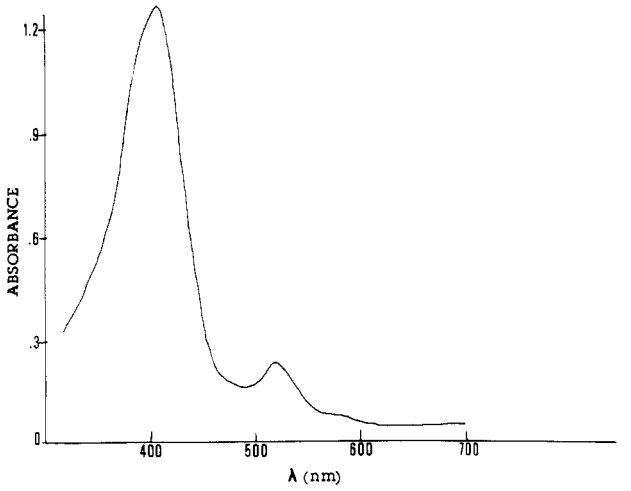

Figure 1. Spectrum of **1** in benzene solution.

in benzene under an inert atmosphere. Such crystals were indefinitely stable in air, but **1** was oxidized in minutes by O_2 in solution.

Magnetic Measurements. Magnetic susceptibility data were collected with a Princeton Applied Research Model 155 vibrating-sample magnetometer (VSM), which was operated from zero field to 1.0 T. The VSM was calibrated with $Hg[Co(NCS)_4]$.[7] Powdered samples of the calibrant and compound **1** were contained in precision-milled Lucite sample holders. Approximately 150 mg of each was used. The temperature at the sample was measured with a GaAs diode, by observing the voltage on a Fluke 8502A 6.5-place digital multimeter. Further details of the techniques, instrumentation, and temperature measurement have been previously described.[8] Corrections for temperature-independent paramagnetism were estimated from tabulated data.[9,10] The diamagnetic correction for TPP^{2-} was taken to be -700×10^{-6}, as suggested by Eaton and Eaton.[11]

EPR Spectra. EPR spectra of powdered samples were obtained on a Bruker ER-220D spectrometer equipped with a variable-temperature unit and microwave frequency counter.

Mössbauer Measurements. The Mössbauer spectrometer was of the constant-acceleration type and was operated in connection with a 256-channel analyzer in the time scale mode. The source was ^{57}Co diffused in rhodium and was kept at room temperature at all times. Spectra were recorded in horizontal transmission geometry, and each run lasted 24 h. Calibration employed the known hyperfine splittings in the metallic iron spectrum, and the isomer shifts reported here are relative to iron metal at room temperature. In calibration experiments with thin iron foils, line widths were typically 0.32 mm s^{-1}. An applied field of 0.13 T transverse to the γ beam was achieved with a permanent magnet. Samples were kept either at 4.2 K (by immersion in He(l)) or at 77 K (by immersion in N_2(l)) for the duration of each run.

X-ray Structure Determination of 1. Crystal data for **1**, together with details pertaining to the X-ray diffraction experiment and subsequent crystallographic calculations, are reported in Table I. Cell constants were obtained by least-squares refinement of the setting angles for 20 reflections ($2\theta_{av} = 21.99°$) on the Nicolet R3m diffractometer.[12] The stability of the crystal was monitored during data collection by measurement of the intensities of 3 standard reflections (105, 63$\bar{4}$, 653) every 200 data points. Over the course of data collection, no significant change in the intensity of any of these reflections was noted. An empirical absorption correction was performed, utilizing intensity profiles obtained as a function of rotation of the diffraction vector. All transmission factors calculated for the complete data set were within 4% of the mean value of the transmission factor. Lorentz and polarization corrections were applied to the data.

Table I. Crystallographic Parameters and Refinement Results

mol formula	$C_{92}H_{56}Fe_2N_{10}S_2 \cdot 2C_6H_6$
mol wt	1633.6
cryst syst	monoclinic
space group	$P2_1/n$
temp, °C	20 (1)
a, Å	14.263 (3)
b, Å	15.184 (4)
c, Å	19.172 (4)
β, deg	93.92 (2)
V, Å^3	4142
Z	2
D(calcd), g cm^{-3}	1.31
cryst dimens, mm	0.14 (001 → 00$\bar{1}$) × 0.54 (010 → 0$\bar{1}$0) × 0.39 (100 → $\bar{1}$00)
radiation	Mo Kα (λ = 0.71073 Å), graphite monochromator
μ, cm^{-1}	4.52
scan type	$\theta/2\theta$
scan speed, deg min^{-1}	variable (2–29)
2θ range, deg	3.5–50
indices collected	$+h,+k,\pm l$
no. of reflections	7320 (4585 with $I > 2\sigma(I)$)
data/parameter ratio	9.7
R	0.068
R_w	0.070
GOF	1.65
g	1.02×10^{-3}
slope, norm prob plot	1.39

Neutral-atom scattering factors[13] with anomalous scattering contributions[14] were employed for all atoms. The position of the unique iron atom was determined by analysis of the Patterson synthesis. Difference Fourier electron density calculations then revealed all atoms of the porphyrin ligand, the unique atoms of the FNT^{2-} bridge, and a benzene molecule that had been incorporated in the lattice during crystallization. The crystallographic inversion center bisected the C(1)–C(1a) bond of the bridging FNT^{2-} ligand. Thus, the asymmetric unit of the unit cell consisted of half of the bridging ligand, an entire $[Fe(TPP)]^+$ unit, and the occluded benzene molecule. During refinement, the site occupancy factor for the atoms of this benzene molecule was allowed to vary; since this factor remained near unity, the value was fixed at 1.00 during the final refinement cycles.

In the final structural model, the carbon atoms of the benzene molecule and the four unique phenyl groups of the TPP^{2-} ligand were refined as rigid hexagons (C–C = 1.395 Å). Hydrogen atoms were included in calculated positions (C–H = 0.96 Å), with each hydrogen atom's isotropic thermal parameter set 20% higher than the equivalent isotropic thermal parameter of the carbon atom to which the hydrogen atom was bound. All non-hydrogen atoms, including those of the rigid groups, were given anisotropic thermal parameters. The refinement converged $((\text{shift/esd})_{av} < 0.010$ over the last five cycles) to yield the discrepancy factors given in Table I. In the final difference electron density map, the maxima and minima were 0.47 and −0.37 e Å^{-3}, respectively.

The final fractional atomic coordinates for all non-hydrogen atoms may be found in Table II. Bond lengths and angles involving the porphyrin core, the iron atom, and the FNT^{2-} ligand may be found in Tables III and IV. Tables of anisotropic thermal parameters (Table SI), calculated hydrogen atom positions (Table SII), selected least-squares planes (Table SIII), and structure factors (observed and calculated, ×10, Table SIV) have been included as supplementary material.

Magnetic Theory

The X-ray diffraction and variable-temperature magnetic susceptibility experiments (see below) show that **1** consists of a FNT^{2-}-bridged iron(III) porphyrin dimer, in which the two iron(III) atoms are magnetically coupled. To account for this observed magnetic interaction, the following theoretical development was undertaken.

The ground state of a high-spin iron(III) ion in an octahedral or square-pyramidal environment is an orbital singlet with a sixfold spin degeneracy. The spin degeneracy is partially removed by spin–orbit coupling admixture of excited states and by low-symmetry crystal field

(7) Brown, D. B.; Crawford, V. H.; Hall, J. W.; Hatfield, W. E. *J. Phys. Chem.* **1977**, *81*, 1303.
(8) Hatfield, W. E.; Weller, R. R.; Hall, J. W. *Inorg. Chem.* **1980**, *19*, 3825.
(9) (a) Figgis, B. N.; Lewis, J. In *Modern Coordination Chemistry*; Lewis, J., Wilkins, R. G., Eds.; Interscience: New York, 1960; Chapter 6, p 403. (b) König, E. *Magnetic Properties of Transition Metal Compounds*; Springer-Verlag: West Berlin, 1966.
(10) Weller, R. R.; Hatfield, W. E. *J. Chem. Educ.* **1979**, *56*, 652.
(11) Eaton, G. R.; Eaton, S. S. *Inorg. Chem.* **1980**, *19*, 1095.
(12) Software used for diffractometer operations was provided with the Nicolet R3m diffractometer. All crystallographic computations were carried out with use of the SHELXTL program library, written by G. M. Sheldrick and supplied by Nicolet XRD Corp. for the Data General Eclipse S/140 computer in the crystallographic laboratory at Colorado State University.
(13) *International Tables for X-ray Crystallography*; Kynoch: Birmingham, England, 1974; Vol. IV, p 99.
(14) *International Tables for X-ray Crystallography*; Kynoch: Birmingham, England, 1974; Vol. IV, p 149.

Table II. Atomic Coordinates ($\times 10^4$) and Thermal Parameters (10^3 Å^2)[a] for [Fe(TPP)]$_2$(μ-FNT-*S*,*S*′)

atom	*x*	*y*	*z*	U_{iso}[b]
Fe	1880 (1)	230 (1)	1309 (1)	44 (1)
S(1)	1491 (1)	393 (1)	119 (1)	67 (1)
N(1)	803 (2)	882 (2)	1743 (2)	46 (1)
N(2)	2664 (2)	1357 (2)	1478 (2)	46 (1)
N(3)	3124 (3)	−457 (2)	1323 (2)	49 (1)
N(4)	1281 (3)	−920 (2)	1611 (2)	50 (1)
N(5)	647 (4)	−1820 (4)	−204 (4)	130 (3)
C(a1)	14 (3)	528 (3)	2014 (3)	51 (2)
C(a2)	685 (3)	1789 (3)	1746 (2)	47 (2)
C(a3)	2291 (3)	2205 (3)	1469 (3)	51 (2)
C(a4)	3614 (3)	1450 (3)	1404 (3)	54 (2)
C(a5)	4026 (3)	−115 (3)	1305 (3)	53 (2)
C(a6)	3210 (3)	−1356 (3)	1242 (3)	53 (2)
C(a7)	1593 (3)	−1760 (3)	1470 (3)	53 (2)
C(a8)	402 (3)	−1033 (3)	1860 (3)	53 (2)
C(b1)	−586 (3)	1231 (3)	2210 (3)	61 (2)
C(b2)	−188 (3)	1987 (3)	2037 (3)	58 (2)
C(b3)	3026 (3)	2819 (3)	1387 (3)	65 (2)
C(b4)	3827 (4)	2377 (3)	1365 (3)	71 (2)
C(b5)	4671 (4)	−814 (3)	1230 (3)	63 (2)
C(b6)	4178 (4)	−1567 (4)	1176 (3)	66 (2)
C(b7)	898 (4)	−2390 (3)	1611 (3)	67 (2)
C(b8)	173 (4)	−1952 (4)	1859 (3)	71 (2)
C(m1)	1346 (3)	2409 (3)	1564 (2)	47 (2)
C(m2)	4256 (3)	774 (3)	1346 (3)	51 (2)
C(m3)	2497 (3)	−1972 (3)	1269 (3)	51 (2)
C(m4)	−179 (3)	−362 (3)	2069 (3)	52 (2)
C(1)	395 (4)	−60 (7)	15 (3)	124 (4)
C(2)	430 (5)	−1139 (4)	−117 (4)	102 (3)
C(11)	1402 (2)	3997 (2)	1957 (2)	67 (2)
C(12)	1078 (2)	4862 (2)	1888 (2)	82 (3)
C(13)	386 (2)	5075 (2)	1365 (2)	85 (3)
C(14)	20 (2)	4424 (2)	911 (2)	92 (3)
C(15)	344 (2)	3560 (2)	980 (2)	75 (2)
C(16)	1035 (2)	3346 (2)	1503 (2)	52 (2)
C(21)	5788 (3)	1290 (3)	1926 (2)	71 (2)
C(22)	6731 (3)	1523 (3)	1898 (2)	90 (3)
C(23)	7156 (3)	1482 (3)	1265 (2)	86 (3)
C(24)	6639 (3)	1208 (3)	660 (2)	91 (3)
C(25)	5696 (3)	975 (3)	688 (2)	83 (3)
C(26)	5271 (3)	1016 (3)	1321 (2)	57 (2)
C(31)	2373 (3)	−3243 (2)	447 (2)	96 (3)
C(32)	2571 (3)	−4112 (2)	271 (2)	118 (4)
C(33)	3070 (3)	−4653 (2)	753 (2)	95 (3)
C(34)	3372 (3)	−4326 (2)	1410 (2)	108 (3)
C(35)	3174 (3)	−3457 (2)	1586 (2)	93 (3)
C(36)	2675 (3)	−2916 (2)	1104 (2)	57 (2)
C(41)	−990 (3)	−930 (3)	3083 (2)	98 (3)
C(42)	−1799 (3)	−1186 (3)	3400 (2)	138 (5)
C(43)	−2672 (3)	−1143 (3)	3028 (2)	135 (5)
C(44)	−2737 (3)	−845 (3)	2338 (2)	150 (5)
C(45)	−1929 (3)	−589 (3)	2021 (2)	115 (4)
C(46)	−1055 (3)	−632 (3)	2394 (2)	65 (2)
C(51)	7202 (14)	6051 (5)	1056 (4)	232 (10)
C(52)	6315 (14)	6391 (5)	857 (4)	254 (12)
C(53)	6233 (14)	7221 (5)	547 (4)	262 (11)
C(54)	7036 (14)	7710 (5)	436 (4)	204 (8)
C(55)	7923 (14)	7370 (5)	635 (4)	198 (8)
C(56)	8005 (14)	6540 (5)	945 (4)	220 (9)

[a] Estimated standard deviations in the least significant digits are given in parentheses. [b] The equivalent isotropic U value for anisotropic atoms is defined as one-third of the trace of the orthogonalized $\mathbf{U}_{ij}$ tensor.

components, resulting in three magnetic doublets characterized by $m_S = \pm^1/_2$, $\pm^3/_2$, and $\pm^5/_2$. The array of multiplets may be described by the spin Hamiltonian (1), which consists of the Zeeman term and the sec-

$$\hat{H} = g\hat{\mathbf{H}}\cdot\hat{\mathbf{s}}\beta + D[\hat{s}_3^2 - {}^1/_3 s(s+1)] \qquad (1)$$

ond-order spin operator.[15] Here s_3 refers to the spin component along the molecular symmetry axis.[15] An isotropic g factor has been assumed,

Table III. Bond Lengths (Å)[a] for [Fe(TPP)]$_2$(μ-FNT-*S*,*S*′)

Fe–S(1)	2.324 (2)	Fe–N(1)	2.052 (4)
Fe–N(2)	2.057 (4)	Fe–N(3)	2.056 (4)
Fe–N(4)	2.045 (4)	S(1)–C(1)	1.708 (7)
N(1)–C(a1)	1.379 (6)	N(1)–C(a2)	1.388 (6)
N(2)–C(a3)	1.393 (6)	N(2)–C(a4)	1.380 (6)
N(3)–C(a5)	1.391 (6)	N(3)–C(a6)	1.381 (6)
N(4)–C(a7)	1.383 (6)	N(4)–C(a8)	1.382 (6)
N(5)–C(2)	1.095 (8)	C(a1)–C(b1)	1.434 (7)
C(a1)–C(m4)	1.384 (7)	C(a2)–C(b2)	1.431 (7)
C(a2)–C(m1)	1.394 (6)	C(a3)–C(b3)	1.419 (7)
C(a3)–C(m1)	1.407 (7)	C(a4)–C(b4)	1.442 (7)
C(a4)–C(m2)	1.385 (7)	C(a5)–C(b5)	1.418 (7)
C(a5)–C(m2)	1.390 (7)	C(a6)–C(b6)	1.431 (7)
C(a6)–C(m3)	1.385 (7)	C(a7)–C(b7)	1.417 (7)
C(a7)–C(m3)	1.408 (7)	C(a8)–C(b8)	1.434 (7)
C(a8)–C(m4)	1.389 (7)	C(b1)–C(b2)	1.333 (7)
C(b3)–C(b4)	1.328 (7)	C(b5)–C(b6)	1.343 (8)
C(b7)–C(b8)	1.342 (8)	C(m1)–C(16)	1.493 (6)
C(m2)–C(26)	1.497 (6)	C(m3)–C(36)	1.493 (6)
C(m4)–C(46)	1.491 (7)	C(1)–C(2)	1.659 (12)
C(1)–C(1a)	1.139 (12)		

[a] Estimated standard deviations in the least significant digits are given in parentheses.

Table IV. Bond Angles (deg)[a] for [Fe(TPP)]$_2$(μ-FNT-*S*,*S*′)

S(1)–Fe–N(1)	102.2 (1)	S(1)–Fe–N(2)	99.0 (1)
N(1)–Fe–N(2)	87.1 (1)	S(1)–Fe–N(3)	102.4 (1)
N(1)–Fe–N(3)	155.3 (1)	N(2)–Fe–N(3)	87.8 (1)
S(1)–Fe–N(4)	107.0 (1)	N(1)–Fe–N(4)	87.6 (1)
N(2)–Fe–N(4)	154.0 (2)	N(3)–Fe–N(4)	86.6 (1)
Fe–S(1)–C(1)	103.1 (2)	Fe–N(1)–C(a1)	128.1 (3)
Fe–N(1)–C(a2)	125.1 (3)	C(a1)–N(1)–C(a2)	106.5 (4)
Fe–N(2)–C(a3)	124.4 (3)	Fe–N(2)–C(a4)	126.6 (3)
C(a3)–N(2)–C(a4)	106.3 (4)	Fe–N(3)–C(a5)	127.5 (3)
Fe–N(3)–C(a6)	125.7 (3)	C(a5)–N(3)–C(a6)	106.1 (4)
Fe–N(4)–C(a7)	125.8 (3)	Fe–N(4)–C(a8)	127.6 (3)
C(a7)–N(4)–C(a8)	105.4 (4)	N(1)–C(a1)–C(b1)	108.9 (4)
N(1)–C(a1)–C(m4)	125.5 (4)	C(b1)–C(a1)–C(m4)	125.5 (4)
N(1)–C(a2)–C(b2)	108.6 (4)	N(1)–C(a2)–C(m1)	125.8 (4)
C(b2)–C(a2)–C(m1)	125.3 (4)	N(2)–C(a3)–C(b3)	109.0 (4)
N(2)–C(a3)–C(m1)	124.8 (4)	C(b3)–C(a3)–C(m1)	126.2 (4)
N(2)–C(a4)–C(b4)	108.5 (4)	N(2)–C(a4)–C(m2)	126.2 (4)
C(b4)–C(a4)–C(m2)	125.2 (4)	N(3)–C(a5)–C(b5)	109.3 (4)
N(3)–C(a5)–C(m2)	125.2 (4)	C(b5)–C(a5)–C(m2)	125.5 (4)
N(3)–C(a6)–C(b6)	109.0 (4)	N(3)–C(a6)–C(m3)	126.2 (4)
C(b6)–C(a6)–C(m3)	124.6 (5)	N(4)–C(a7)–C(b7)	110.3 (4)
N(4)–C(a7)–C(m3)	125.3 (4)	C(b7)–C(a7)–C(m3)	124.3 (4)
N(4)–C(a8)–C(b8)	109.3 (4)	N(4)–C(a8)–C(m4)	125.6 (4)
C(b8)–C(a8)–C(m4)	125.1 (5)	C(a1)–C(b1)–C(b2)	107.8 (5)
C(a2)–C(b2)–C(b1)	108.2 (4)	C(a3)–C(b3)–C(b4)	108.3 (5)
C(a4)–C(b4)–C(b3)	107.9 (5)	C(a5)–C(b5)–C(b6)	107.8 (5)
C(a6)–C(b6)–C(b5)	107.8 (5)	C(a7)–C(b7)–C(b8)	107.4 (5)
C(a8)–C(b8)–C(b7)	107.6 (5)	C(a2)–C(m1)–C(a3)	123.7 (4)
C(a2)–C(m1)–C(16)	117.4 (4)	C(a3)–C(m1)–C(16)	118.8 (4)
C(a4)–C(m2)–C(a5)	124.8 (4)	C(a4)–C(m2)–C(26)	117.8 (4)
C(a5)–C(m2)–C(26)	117.4 (4)	C(a6)–C(m3)–C(a7)	123.0 (4)
C(a6)–C(m3)–C(36)	120.2 (4)	C(a7)–C(m3)–C(36)	116.7 (4)
C(a1)–C(m4)–C(a8)	124.6 (4)	C(a1)–C(m4)–C(46)	118.5 (4)
C(a8)–C(m4)–C(46)	116.9 (4)	S(1)–C(1)–C(2)	112.3 (5)
S(1)–C(1)–C(1a)	146.7 (14)	C(2)–C(1)–C(1a)	101.0 (11)
N(5)–C(2)–C(1)	165.3 (8)	C(m1)–C(16)–C(11)	122.0 (2)
C(m1)–C(16)–C(15)	118.0 (2)	C(m2)–C(26)–C(21)	120.3 (2)
C(m2)–C(26)–C(25)	119.7 (2)	C(m3)–C(36)–C(31)	119.1 (2)
C(m3)–C(36)–C(35)	120.8 (2)	C(m4)–C(46)–C(41)	118.8 (2)
C(m4)–C(46)–C(45)	121.2 (2)		

[a] Estimated standard deviations in the least significant digits are given in parentheses.

and the higher order spin operators (as well as lower symmetry terms) have been ignored, since it is known from EPR studies that the D term is predominant for the majority of iron(III) compounds.[16] In the absence of a magnetic field, the doublets will have the energies $-8D/3$, $-2D/3$,

(15) Carrington, A.; McLachlan, A. D. *Introduction to Magnetic Resonance*; Harper and Row: New York, 1967.

(16) Bencini, A.; Gatteschi, D. In *Transition Met. Chem. (N.Y.)* **1982**, *8*, 1–178.

and $10D/3$. In addition to giving rise to anisotropy in the EPR spectrum, the splittings, if large, affect the bulk magnetic properties significantly, especially at low temperatures.

The spin Hamiltonian may be transformed to the laboratory coordinate frame $[x, y, z]$:

$$\hat{H}^{(j)} = g\beta H_z\hat{s}_z + D[\hat{s}_z^2 - \tfrac{1}{3}s(s+1)](3\cos^2\theta - 1)/2 + D\sin^2\theta\,(\hat{s}_x^2 - \hat{s}_y^2)/2 + D\sin\theta\cos\theta\,(\hat{s}_x\hat{s}_z + \hat{s}_z\hat{s}_x) \quad (2)$$

The superscript j refers to the magnetic ion at site j, and θ denotes the orientation of the complex relative to the magnetic field direction.

The spin Hamiltonian was diagonalized within the basis set $|^5/_2\rangle$, $|^3/_2\rangle$, $|^1/_2\rangle$, $|^{-1}/_2\rangle$, $|^{-3}/_2\rangle$, and $|^{-5}/_2\rangle$, yielding six eigenvalues, W_i, and the corresponding eigenvectors, $|i\rangle$. The magnetic susceptibility was then calculated by using (3). As a result of the transformation, only the

$$\chi^{(j)}(\theta) = \frac{N}{H}\frac{\sum_i^K\left[-\frac{\partial W_i}{\partial H}\exp\left(-\frac{W_i}{kT}\right)\right]}{\sum_i^K\exp\left(-\frac{W_i}{kT}\right)} \quad (3)$$

diagonal matrix elements of $H^{(j)}$ are field-dependent, and $\delta W_i/\delta H$ can be expressed as $\{g\beta\langle i|s_z|i\rangle\}$.[17] To account for the random distribution of molecular axes, the susceptibility of a powdered sample was calculated from (4) by numerical integration. Calculations were typically made for

$$\chi_{av} = \int \chi^{(j)}(\theta)\,d(\cos\theta) \quad (4)$$

six directions. Effective magnetic moments were calculated from

$$\mu_{eff} = 2.828(\chi_M T)^{1/2}$$

This theory for isolated Fe(III) ions was unable to describe the magnetic properties of **1** with realistic parameters.

In the presence of an isotropic exchange interaction between two ions for which $s_1 = s_2 = {}^5/_2$, the energy levels of the pair may be described by the spin Hamiltonian

$$\hat{\mathbf{H}} = \hat{\mathbf{H}}^{(1)} + \hat{\mathbf{H}}^{(2)} - 2J_{12}\hat{\mathbf{s}}_1\cdot\hat{\mathbf{s}}_2 \quad (5)$$

The basis set of wave functions corresponding to the $(2s_1 + 1)(2s_2 + 1)$ states of the pair have been tabulated by Owen.[18] In that treatment, the two exchange-coupled ions were assumed to be magnetically equivalent, with their symmetry axes coincident with the vector connecting the two sites. The magnetic properties of an exchange-coupled pair of $s = {}^5/_2$ ions in the presence of a large zero-field splitting and anisotropic g factors have been treated by Owen and Harris[19a] and by Laskowski and Hendrickson.[19b] All of the non-zero matrix elements were explicitly calculated for $\mathbf{H}^{(1)} = \mathbf{H}^{(2)}$, the matrix was diagonalized, and the magnetic susceptibility was calculated as a function of g, J, and D.

In the present work, the matrix elements were calculated as follows. A two-dimensional matrix representation of each state vector

$$|S,M\rangle = \sum_{m_1m_2} C_{m_1m_2}^{SM}|m_1m_2\rangle$$

was applied according to the algorithm

$$\langle S'M'|\hat{\mathbf{H}}^{(1)} + \hat{\mathbf{H}}^{(2)}|SM\rangle = \sum_{m_1'm_2'} c_{m_1'm_2'}^{S'M'}\left[\sum_{m_1} H_{m_1'm_1}c_{m_1m_2'}^{SM} + \sum_{m_2} c_{m_1'm_2}^{SM}H_{m_2'm_2}\right]$$

where $H_{m_1'm_1} = \langle m_1'|\mathbf{H}^{(1)}|m_1\rangle$. After the addition of diagonal terms

$$\langle SM|-2J\mathbf{s}_1\cdot\mathbf{s}_2|SM\rangle = -JS(S+1) + 35J/2$$

for isotropic exchange, the matrix elements $\langle S'M'|H|SM\rangle$ were obtained. In this manner, a more general situation, i.e., for the case in which $\mathbf{H}^{(1)}$ and $\mathbf{H}^{(2)}$ are not identical, can easily be treated. The procedure is also advantageous when the single-ion Hamiltonian is expressed in the laboratory frame, as implied by eq 2. The total 36×36 matrix of the Hamiltonian was arranged in terms of the coupled spin components in the order $|5,5\rangle$, $|5,4\rangle$, $|4,4\rangle$, $|5,3\rangle$, $|4,3\rangle$, ..., $|4,-4\rangle$, $|5,-4\rangle$, $|5,-5\rangle$. Such an arrangement results in a block-diagonal form of the matrix and allows a test to be made with $J = 0$ and $D \neq 0$. The magnetic susceptibility of the pair of exchange-coupled iron(III) ions may be calculated with eq 3 with $K = 36$ and subsequently spatially averaged (to account for the random distribution of molecular axes in the powdered sample) with eq 4. When no exchange is present, calculations with either approach, i.e., for the monomer or for the pair, yield identical magnetic susceptibilities.

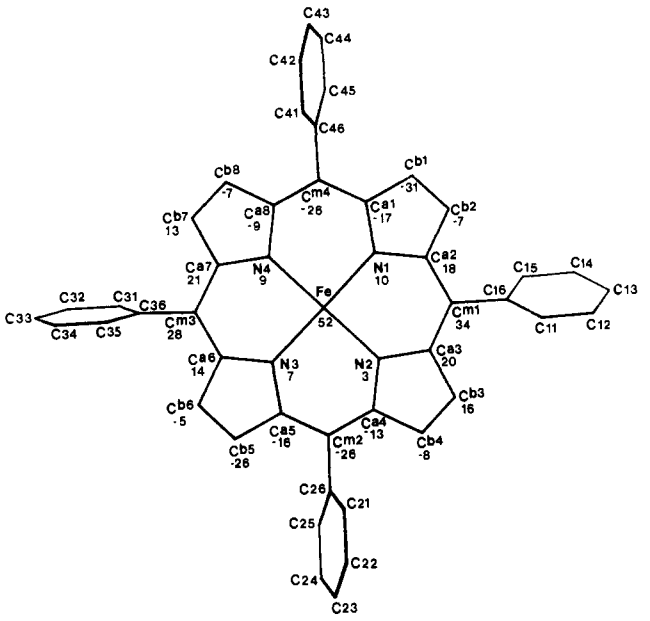

Figure 2. Numbering scheme for the $[Fe(TPP)]^+$ unit of **1**. Also shown are distances above and below the best plane through the atoms of the porphyrin core ($\times 10^2$ Å).

Results

Crystal Structure of 1. Figure 2 illustrates the numbering scheme for the porphyrin ligand and the deviations of individual atoms from the 24-atom plane of the porphyrin core. The metric parameters for the iron atom and the porphyrin core (Fe–N(av) = 2.053 (2) Å, N···Ct_N(av) = 2.003 Å, N···Ct_P(av) = 2.004 Å, Fe···Ct_P = 0.52 Å, and Fe···Ct_N = 0.45 Å) correspond well with the values expected for five-coordinate, high-spin Fe(III).[20] Although the average Fe–N distance is slightly shorter than Fe(III)–N distances previously observed in high-spin iron(III) porphyrin complexes (2.060 (3)–2.087 (8) Å), it is not as short as the Fe(III)–N bond lengths in porphyrin complexes involving intermediate- and low-spin iron(III) atoms. The N···Ct_P distance is very slightly smaller than the distance of 2.010 Å typical of a "strain-free" porphyrin.[21] This shrinking of the core is accomplished through a slight S_4 ruffling (see Figure 2). The individual pyrrole rings involving N1–4 make angles of 12.1, 9.1, 10.2, and 8.3°, respectively, with the mean porphyrin plane. The mean porphyrin core bonding parameters are, given the core size, not exceptional: N–C_a = 1.385 (5) Å, C_a–C_b = 1.428 (9) Å, C_a–C_m = 1.373 (7) Å, C_a–N–C_a = 106.1 (5)°, N–C_a–C_b = 109.1 (6)°, N–C_a–C_m = 125.6 (5)°, C_b–C_a–C_m = 125.2 (6)°, C_a–C_b–C_b = 107.9 (3)°, and C_a–C_m–C_a = 124.0 (3)°.

The X-ray diffraction experiment unambiguously establishes the bridging nature of the *trans*-1,2-dicyanoethylenedithiolate dianion (FNT^{2-}). The fully refined structural model, however, exhibits chemically unreasonable bond lengths for the FNT^{2-} ligand: C(1)–C(1a) = 1.14 (1) Å (a C–C double bond) and C(1)–C(2) = 1.65 (1) Å (a C-C single bond). The atoms of this bridging ligand are executing high-amplitude thermal motion (see Figure 3), which is apparently poorly modeled by the standard anisotropic thermal tensor. An attempt to analyze this motion using a librational model[22] for the FNT^{2-} ligand did not result in a reasonable fit. An alternative model in which all the atoms of the bridging group were given isotropic thermal parameters showed, at convergence, extraneous peaks ($\sim$1 e Å^{-3}) in the vicinity of the atoms in the bridge. Treatment of the FNT^{2-}

(17) (a) Marathe, V. R.; Mitra, S. *Chem. Phys. Lett.* **1974**, *27*, 104. (b) Vermaas, A.; Groeneveld, W. L. *Chem. Phys. Lett.* **1974**, *27*, 583.
(18) Owen, J. *J. Appl. Phys., Suppl.* **1961**, *32*, 213.
(19) (a) Owen, J.; Harris, E. A. In *Electron Paramagnetic Resonance*; Geschwind, S., Ed.; Plenum: New York, 1972; p 446ff. (b) Laskowski, E.; Hendrickson, D. N. *Inorg. Chem.* **1978**, *17*, 457.
(20) Scheidt, W. R.; Reed, C. A. *Chem. Rev.* **1981**, *81*, 543.
(21) Hoard, J. L. *Ann. N.Y. Acad. Sci.* **1973**, *206*, 18.
(22) Schomaker, V.; Trueblood, K. N. *Acta Crystallogr., Sect. B: Struct. Crystallogr. Cryst. Chem.* **1968** *B24*, 63.

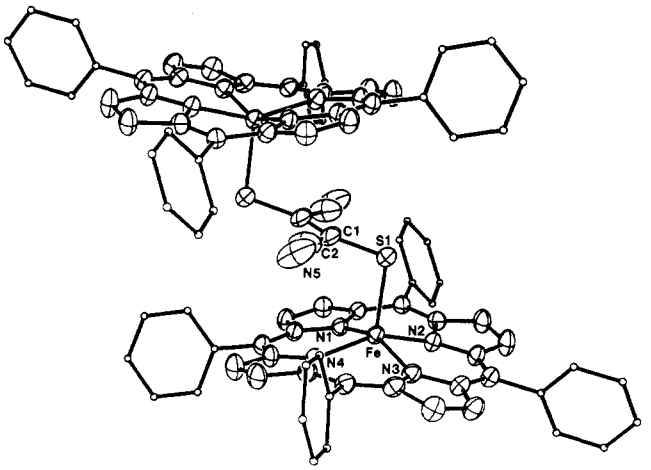

Figure 3. View of the FNT^{2-}-bridged dimeric unit of **1**. Thermal ellipsoids are drawn at the 30% probability level, carbon atoms of the phenyl rings have been drawn as spheres of arbitrary radius for clarity, and hydrogen atoms have been omitted.

bridging ligand as a rigid, idealized group was considered but rejected, on the grounds that this would mask meaningful changes in structure just as severely as the inadequate thermal motion model. Since no structural model was clearly superior, all results reported herein are taken from the completely anisotropic refinement.

The atoms of the bridging FNT^{2-} ligand are coplanar to within 0.01 Å; this plane makes an angle of 17° with respect to the mean porphyrin plane. If the FNT^{2-} ligand is to function as a bridging unit between two parallel porphyrin molecules, it must adopt an orientation parallel or nearly parallel to the porphyrin planes, as is seen for **1**; a perpendicular orientation would result in strong steric conflicts between the cyano groups and atoms of the porphyrin cores. This geometry implies that the bonding of the sulfur atoms to the iron atoms must involve electrons from the π system of the FNT^{2-} ligand. Due to the poorly modeled motion of the bridging FNT^{2-} ligand, the consequences of this type of interaction on the bond distances within the ligand cannot be evaluated. The trans geometry and the orientation of the bridging ligand require that the two porphyrin cores be "slipped" with respect to each other, and the intramolecular Fe–Fe distance is long (7.126 (1) Å) as a consequence.

The bond distances previously observed between sulfur (thiolate, thioether, and hydrosulfido ligands)[3] and the iron atoms of a variety of porphyrins have been surprisingly similar (2.298 (3)–2.370 (3) Å) despite variations in the oxidation state, spin state, and/or coordination number of the iron atom. The Fe–S distance in **1** (2.324 (2) Å) falls within the range of distances exhibited by these Fe–S porphyrin systems. Only in (TBA)-$\{[Fe(p\text{-Cl-TPP})]_2[Cu(MNT)_2]_2\}\cdot 3C_6H_6$,[23] where the bridging sulfur atoms of MNT^{2-} ligands are simultaneously bound to an iron(III) atom and a copper(II) atom, are exceptionally long Fe–S distances observed (Fe–S = 2.444 (2), 2.549 (2) Å).

The dihedral angles between the phenyl groups of the TPP^{2-} ligand and the mean porphyrin plane (phenyl 1, 63°; phenyl 2, 74°; phenyl 3, 80°; phenyl 4, 76°) vary but do not seem to be correlated with the placement of the bridging FNT^{2-} ligand or the relative positions of the porphyrin cores in the dimeric unit.

EPR and Mössbauer Spectra. Figure 4 shows the X-band EPR spectrum of a powdered sample of **1** at 7.8 K. The spectrum is typical of $S = {}^5/_2$ heme iron with significant rhombic distortion of the ligand field. As expected for a case with a large zero-field splitting of 9.6 cm^{-1} (see below), resonances were observed near $g = 2$ and $g = 6$.

The Mössbauer spectrum of **1** was recorded at 4.2 and 77 K, both with and without an applied magnetic field of 130 mT. In all cases, the Mössbauer spectrum showed a quadrupole doublet,

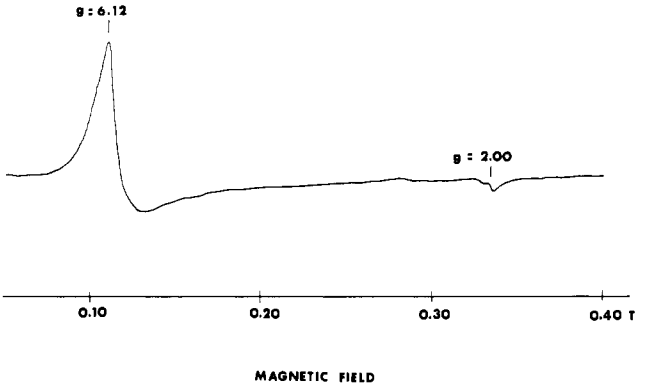

Figure 4. EPR spectrum of a powdered sample of **1** at 7.8 K.

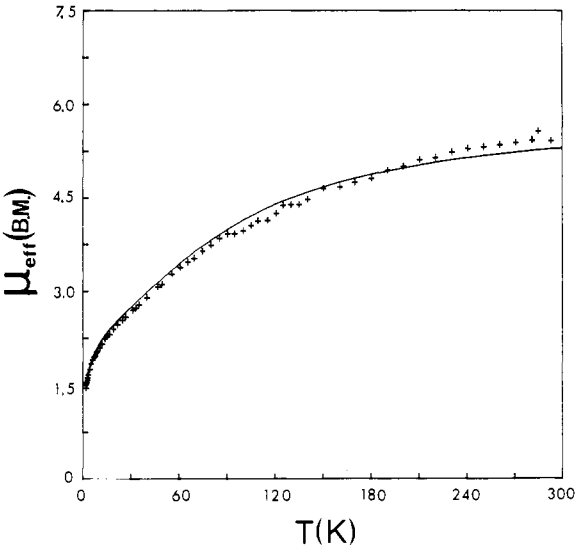

Figure 5. Temperature dependence of the effective magnetic moment of a powdered sample of **1**. The best fit (solid line) was obtained with $J = -8.5$ cm^{-1} and $D = 9.6$ cm^{-1}, with g held constant at 2.0.

with no visible differences between the spectra taken with and those taken without the applied field. There was no evidence of the broad lines or long tails on the absorption lines that often characterize spin–spin relaxation effects in Fe(III).

At 4.2 K, the quadrupole splitting and isomer shift (with respect to metallic Fe) were $\Delta E = 0.80$ mm s^{-1} and $\delta = 0.41$ mm s^{-1}; at 77 K the corresponding values were $\Delta E = 0.80$ mm s^{-1} and $\delta = 0.42$ mm s^{-1}. The lack of temperature dependence in the value of ΔE, as well as the sizes of the quadrupole splitting and the isomer shift, is consistent with a formal assignment of high-spin iron(III) character to each metal center.

The question of spin coupling is addressed by comparing the Mössbauer spectrum of **1** in zero field with that of **1** in the applied field. A magnetic field of 130 mT at 4.2 K is expected to exhibit differences over the zero-field spectrum if the iron atoms are paramagnetic with half-integral spin. On the other hand, integral-spin paramagnetic iron is not readily perturbed by an applied magnetic field (unless the field exceeds 1 T). The apparent lack of perturbation of the Mössbauer spectrum by a relatively small applied field is consistent with the interpretation that the iron centers are spin-coupled, giving rise to integral spin density at each iron atom.

Magnetic Susceptibility. In the analysis of the experimental magnetic susceptibility data for **1**, the g factor was kept constant at 2.0, and both the zero-field parameter D and the isotropic exchange coupling constant J were allowed to vary freely in a nonlinear Simplex[24] least-squares fitting procedure. The criterion for the best fit was the minimum value of the function

(23) Schauer, C. K.; Akabori, K.; Elliott, C. M.; Anderson, O. P. *J. Am. Chem. Soc.* **1984**, *106*, 1127.

(24) (a) Spendley, W.; Hext, G. R.; Himsworth, F. R. *Technometrics* **1962**, *4*, 441. (b) Nelder, J. A.; Mead, R. *Computer J.* **1965**, *7*, 308.

$$F = \sum_i (\chi_i^{obsd} - \chi_i^{calcd})^2 / (\chi_i^{obsd})^2$$

Optimum values of the parameters were $J = -8.5$ cm^{-1} and $|D| = 9.6$ cm^{-1}. The solid line in Figure 5 was calculated by using these optimum parameters.

The sign of D was not determined. The evaluation of the zero-field splitting parameter from low-temperature magnetic susceptibility data for $S = {}^5/_2$ systems has been discussed by several authors.[25,26] The limitations of the practice are well-recognized, especially in the presence of magnetic exchange interactions. Calculations with various ratios of J/D confirm that it will be possible to determine the sign of D from average magnetic susceptibility data only in fortuitous circumstances.

Discussion

Consideration of the crystal packing in **1** indicates that there is little or no opportunity for π overlap between neighboring nonlinked porphyrins, and the distance between nonbridged nearest-neighbor iron atoms is large (8.97 Å). Given these facts, it is likely that a major portion of the magnetic interaction is occurring through the bridging FNT^{2-} ligand. The orientation of the FNT^{2-} ligand relative to the porphyrin plane implies that the magnetic interaction is occurring largely through the FNT^{2-} π system.

In both **1** and the related compound (TBA){[Fe(*p*-Cl-TPP)]$_2$[Cu(MNT)$_2$]$_2$}·3C$_6$H$_6$[23] (hereafter **2**), the bonds between iron and sulfur are approximately perpendicular to the planes of the bridging FNT^{2-} and MNT^{2-} ligands. This is in contrast to the normal chelating mode for MNT^{2-}, in which bonding to a metal atom occurs in the plane of the ligand. The fact that the Fe-S bond distance in **1** is very similar to the Fe-S distances observed for other thiolate and thioether complexes of iron porphyrins demonstrates that the long Fe-S distances characteristic of **2** are not due to the unusual binding geometry of the MNT^{2-} ligand. Instead, these "abnormal" distances must be a consequence of the simultaneous interaction of the bridging sulfur atoms of the MNT^{2-} ligands with the copper(II) ion and with the iron(III) atoms of the porphyrin units. Since **1** contains high-spin iron(III) atoms, the influence of the copper(II) atom on the Fe-S bonding in **2** must also be responsible for the intermediate-spin ($S = {}^3/_2$) state inferred from the structural results for the five-coordinate Fe(III) atom in **2**. All other five-coordinate ferric porphyrins with axial sulfur ligand atoms are high spin, with the exception of the recently characterized low-spin (hydrosulfido)(5,10,15,20-tetrakis(4-methoxyphenyl)porphinato)iron(III) complex.[3f] Thus, the presence of the copper(II) atom in **2** is apparently responsible for both the longer Fe-S bond length *and* the unusual spin state.

Acknowledgment. C.M.E. and O.P.A. thank the National Institutes of Health (Grant No. GM-30306) and the Biomedical Research Support Grant Program at Colorado State University for generous support of this work. The Nicolet R3m/E diffractometer and computing system at Colorado State University were purchased with funds provided by the National Science Foundation (Grant No. CHE 8103011). W.E.H. thanks the National Science Foundation for support (Grant No. CHE8308129).

Registry No. **1**, 101248-27-5; Fe(TPP)(ClO$_4$), 57715-43-2.

Supplementary Material Available: Anisotropic thermal parameters for **2** (Table SI), calculated hydrogen atom positions (Table SII), selected least-squares planes (Table SIII), and observed and calculated structure factors (×10, Table SIV) (32 pages). Ordering information is given on any current masthead page.

(25) Kotani, M. *Adv. Chem. Phys.* **1964**, *7*, 159.
(26) Mitra, S. In *Iron Porphyrins*; Lever, A. B. P., Gray, H. B., Eds.; Addison-Wesley: Reading, MA, 1983; Vol. 2.

Contribution from the Department of Chemistry, State University of New York at Stony Brook, Stony Brook, New York 11794

Gallium Analogues of Iron-Sulfide-Thiolate Compounds. Analysis of the Structural Parameters in Gallium(III) and Iron(III) Chalcogenide Compounds[1]

Lynn E. Maelia and Stephen A. Koch*

Received December 26, 1985

Several gallium-sulfide-thiolate compounds that are structural analogues of the well-known Fe(III)-S^{2-}-RS^- complexes have been prepared and structurally characterized. Crystalline $[Ga(SR)_4]^-$ complexes (SR = SMe, SEt, S-*i*-Pr, SPh, S-2,3,5,6-Me$_4$C$_6$H, S-2,4,6-(*i*-Pr)$_3$C$_6$H$_2$) have been prepared by the reaction of either $GaCl_3$ or $[GaCl_4]^-$ with 5 equiv of LiSR. The $[Ga(SR)_4]^-$ compounds were frequently isomorphous with the corresponding $[Fe(SR)_4]^-$ complex. The structures of $[(n\text{-}Pr)_4N][Ga(SEt)_4]$ (**1**) and $[Et_4N][Ga(SPh)_4]$ (**2**) were determined by X-ray crystallography. Data for **1**: tetragonal, $I\bar{4}$ space group, with $Z = 2$, $a = b = 10.643$ (3) Å, $c = 12.433$ (2) Å, and $V = 1408$ (1) Å^3. Data for **2**: orthorhombic, $P2_12_12_1$ space group, with $Z = 4$, $a = 11.449$ (3) Å, $b = 11.540$ (3) Å, $c = 24.50$ (1) Å, and $V = 3237$ (4) Å^3. The GaS_4 core of **1** has nearly perfect T_d symmetry, and Ga-S = 2.264 (3) Å. There are two distinctive conformations of the thiolate ligands in the $[Ga(SPh)_4]^-$ anion of **2**. $[Et_4N]_2[Ga_2S_2(SPh)_4]$ (**3**), which is an analogue of the FeS compound $[Fe_2S_2(S\text{-}p\text{-}tol)_4]^{2-}$ (**4**), has been synthesized and structurally characterized. Data for **3**: monoclinic, $P2_1/n$ space group, with $Z = 2$, $a = 11.359$ (3) Å, $b = 12.745$ (2) Å, $c = 15.411$ (1) Å, $\beta = 93.56$ (2)°, and $V = 2227$ (1) Å^3. The structures of **3** and **4** and related solid-state compounds have been analyzed in the context of a general discussion of the geometric parameters of edge-sharing tetrahedra.

Introduction

Some similarities in the coordination chemistry of gallium(III) and high-spin iron(III) have long been recognized to result from their similar charges and ionic radii.[2] Because of the biological importance of iron-sulfur proteins,[3] Fe(III)-thiolate and iron-sulfide-thiolate complexes have been extensively investigated.[4] We wish to report some studies that indicate that gallium will have an analogous chemistry and that gallium-sulfide clusters will be valuable for an increased understanding of the structure/electronic structure relationships in iron-sulfur compounds. Although solid-state gallium chalcogenide compounds have come

(1) Maelia, L.; Koch, S. A. Presented in part at the 188th National Meeting of the American Chemical Society, Philadelphia, PA, 1984; paper INOR 156.
(2) Sheka, I. A.; Chaus, I. S.; Mityureva, T. T. *The Chemistry of Gallium*; Elsevier: Amsterdam, 1966. Mikheeva, L. M.; Grigor'ev, A. N. *Russ. J. Inorg. Chem.* (*Engl. Transl.*) **1984**, *29*, 241-244.
(3) Lovenberg, W., Ed. *Iron-Sulfur Proteins*; Academic: New York, 1973; Vol. I and II. *Ibid.* 1977; Vol. III. Spiro, T. G., Ed. *Metal Ions in Biology*; Wiley-Interscience: New York, 1982; Vol. 4.
(4) Berg, J. M.; Holm, R. H. In *Metal Ions in Biology*; Spiro, T. G., Ed.; Wiley-Interscience: New York, 1982; Vol. 4, Chapter 1.

0020-1669/86/1325-1896$01.50/0